Structural Implications of Hydrogen-Bond Energetics in Membrane Proteins Revealed by High-Pressure Spectroscopy

Arvi Freiberg,[†‡*] Liina Kangur,[†] John D. Olsen,[§] and C. Neil Hunter[§]
[†]Institute of Physics and [‡]Institute of Molecular and Cell Biology, University of Tartu, Estonia; and [§]Department of Molecular Biology and Biotechnology, University of Sheffield, Sheffield, United Kingdom

ABSTRACT The light-harvesting 1 (LH1) integral membrane complex of *Rhodobacter sphaeroides* provides a convenient model system in which to examine the poorly understood role of hydrogen bonds (H-bonds) as stabilizing factors in membrane protein complexes. We used noncovalently bound arrays of bacteriochlorophyll chromophores within native and genetically modified variants of LH1 complexes to monitor local changes in the chromophore binding sites induced by externally applied hydrostatic pressure. Whereas membrane-bound complexes demonstrated very high resilience to pressures reaching 2.1 GPa, characteristic discontinuous shifts and broadenings of the absorption spectra were observed around 1 GPa for detergent-solubilized proteins, in similarity to those observed when specific (α or β) H-bonds between the chromophores and the surrounding protein were selectively removed by mutagenesis. These pressure effects, which were reversible upon decompression, allowed us to estimate the rupture energies of H-bonds to the chromophores in LH1 complexes. A quasi-independent, additive role of H-bonds in the α- and β-sublattices in reinforcing the wild-type LH1 complex was established. A comparison of a reaction-center-deficient LH1 complex with complexes containing reaction centers also demonstrated a stabilizing effect of the reaction center. This study thus provides important insights into the design principles of natural photosynthetic complexes.

INTRODUCTION

Integral membrane proteins constitute about one third of the total number of proteins in any organism. They are responsible for energy production, transport, signaling, and many other crucial life-supporting functions. Correct protein function is dependent upon the protein's folded structure (1), which is a product of various weak forces, such as hydrophobic interactions, hydrogen bonds (H-bonds), and salt bridges, acting in concert. H-bond interactions play a role in binding of cofactors in enzymes and basepairing interactions between the strands of DNA, and are responsible for the elasticity of skeletal and cardiac muscles. An H-bonding network has also been shown to play a catalytic role in photosynthetic oxygen evolution (2). Although there is no doubt that H-bonds are extremely important structural elements of all basic biomolecules, their energetics and precise role in stabilizing proteins are still matters of debate (3).

The H-bond energies in simple model compounds and small peptides have been investigated in great detail (4,5). However, this is not the case for folded globular proteins, and especially membrane proteins, where individual H-bonds are much more difficult to characterize (3,6). Scanning calorimetry and titration with chemical denaturants such as urea are commonly used to study protein H-bond energies, but because they probe the unfolding of the whole protein, they do not usually yield bond-specific information. Moreover, scanning the temperature at constant pressure, as in calorimetry, causes simultaneous changes of the system's energy and its volume/density that are difficult to separate. Denaturants are often chemically active and may also modify the chemical potential of the solute. For these reasons, the use of another fundamental thermodynamic variable, pressure, rather than temperature, is an attractive alternative. Continuous and reversible tuning of the density of proteins can be achieved over a wide range without appreciably changing the primary structure of the proteins, which is determined by strong, stable covalent bonds. However, H-bonds that play important roles in the secondary and tertiary structures of the proteins are reported to be either widely insensitive to pressure (7) or promoted by it (8).

To date, mainly water-soluble globular proteins have been studied under high pressures, with the result that functional protein structures cover just a narrow region in the phase diagram around physiological temperatures (8–11). To obtain detailed information about the structural role of H-bonds on an integral membrane protein, we studied light-harvesting (LH) complexes of purple photosynthetic bacteria, which are some of the best-characterized membrane chromoproteins. In phototrophic bacteria such as *Rhodobacter sphaeroides*, peripheral LH2 complexes donate energy to the LH1 complexes, which encircle the reaction centers (RCs), forming a core RC-LH1 complex. In the RCs, the excitation energy is transformed into potential chemical energy. Low-resolution structural models of core complexes have been obtained for a number of species (12–15,16). In this work, we used the intrinsic bacteriochlorophyll *a* (BChl) chromophores of the LH1 complex as spatially local and sensitive optical probes to identify and study the energetics of individual H-bonds that undergo

Submitted September 5, 2012, and accepted for publication October 23, 2012.

*Correspondence: arvi.freiberg@ut.ee

Editor: Leonid Brown.

0006-3495/12/12/2352/9 $2.00

http://dx.doi.org/10.1016/j.bpj.2012.10.030

major changes under externally applied high pressure. The basic building block for in vivo assembly of the LH1 complex is a $\alpha\beta$-$BChl_2$ heterodimer of membrane-spanning α-helical α- and β-apoproteins, with each apoprotein noncovalently binding one BChl molecule (17) (see Fig. 1). The organization of bacterial core complexes can vary, and consists of 15 (13), 16 (18), or 28 (14) such dimeric structural elements. In wild-type (WT) *Rba. sphaeroides*, open *C*- or *S*-shaped antenna structures encircling one or two RCs in planar or nonplanar geometry are known to coexist in photosynthetically grown cells (19).

The LH membrane complexes were first investigated under high pressure in (20). Subsequent studies (21–23) showed that increasing the pressure at laboratory temperatures up to ~500 MPa generally caused a smooth red shift (i.e., to lower energy) and broadening of the near-infrared absorption bands of BChl. Past 500 MPa, however, a nonmonophasic behavior was observed in LH2 complexes purified with mild detergents into a detergent-buffer environment, which was interpreted as arising from rupture of the H-bonds at the binding sites of the strongly excitonically coupled B850 BChls (24,25). Here, we extended this approach by examining a series of WT and genetically engineered variants of the core complex (see Fig. 1), including an LH1-only complex, an RC-LH1 monomer complex, a mixture of the monomer and dimer RC-LH1-PufX complexes, and two point mutations of the RC-LH1-PufX complexes that eliminate the H-bonds to specific Bchls at positions α+11 and β+9. Due to the multimeric nature of these complexes, where each WT $\alpha\beta$-$BChl_2$ subunit has two relevant H-bonds, the total number of H-bonds per complex is large: 32 in LH1-only and RC-LH1, 56 in WT RC-LH1-PufX dimer, and 28 in RC-LH1-PufX monomer. The α+11 or β+9 mutants will have half the number of H-bonds of the equivalent WT complex. It has already been established by site-directed mutagenesis that H-bonding tunes the BChl absorbance that is responsible for the lowest-energy B875 exciton band in LH1 complexes (26–30). In this work, we examined the structural stabilization and absorbance tuning roles of H-bonds in detergent-isolated and native membrane-embedded LH1 antenna complexes using hydrostatic pressures that reached 2100 MPa. By showing that pressure-induced breakage of H-bonds produced reversible spectral effects, we were able to quantify the average rupture energies for these bonds in the BChl binding sites.

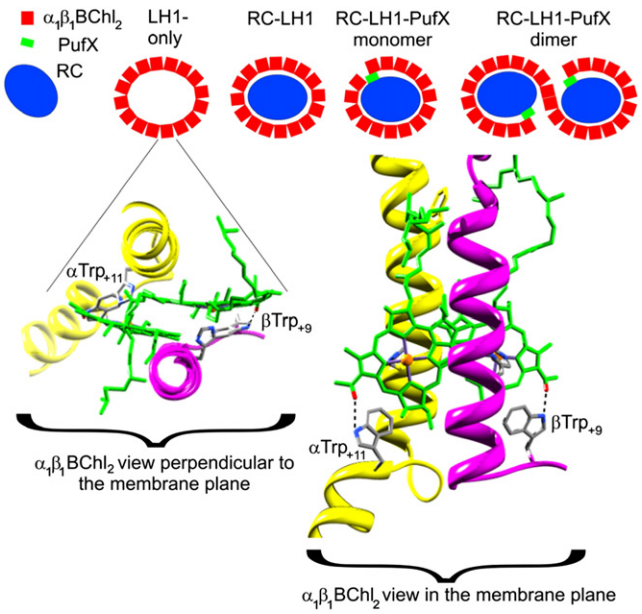

FIGURE 1 Diagrammatic representation of the studied LH complexes. Each red square represents the $\alpha\beta$-$BChl_2$ heterodimer building block of the LH1 complex. Below are two views of the $\alpha\beta$-$BChl_2$ subunit based on the atomic structure of the LH2 complex from *Phaeospirillum molischianum*, together with mutagenesis, atomic force microscopy, and cryoelectron microscopy data (14,15,25,26). The two residues that have been altered from Trp to Phe in the αTrp$_{+11}$ and βTrp$_{+9}$ mutants are in stick representation, and the rest of the transmembrane polypeptides are depicted as a ribbon. The Bchls and the H-bond partners are also shown.

MATERIALS AND METHODS

Materials

The DD13 deletion strain of *Rba. sphaeroides* (31), which was manipulated to remove the genes encoding the LH2, LH1, and RC complexes, was complemented with plasmid-borne copies of the *puf BALMX* genes to produce photosystems containing LH1-only, monomeric RC-LH1, or dimeric RC-LH1-PufX complexes. Further point mutations were introduced into either *pufA* or *pufB* encoding LH1 α- and β-apoproteins, respectively. One of these mutations, αTrp$_{+11}$Phe, alters the tryptophan that H-bonds to the *C*3 acetyl carbonyl group (IUPAC numbering) of one of the BChls in the $\alpha\beta$-$BChl_2$ structural unit (26,28), and the other, βTrp$_{+9}$Phe, disrupts the H-bond to the *C*3 acetyl carbonyl group of the other BChl (28). Double-mutant complexes with replacements in both sites are structurally compromised and are unstable in detergent even at ambient temperature and pressure. LH membranes and purified complexes were prepared according to published methods and stored at liquid nitrogen temperature. The samples were thawed before the experiments and diluted with 20 mM HEPES, pH 7.5 buffer to obtain an optical density of ~0.3 at 875 nm, the absorption maximum, in the assembled pressure cell. The buffering ability of HEPES is preserved over a broad temperature and pressure range. The buffer for isolated complexes additionally contained the detergent dihexanoylphosphatidylcholine (DHPC). Above a critical micelle concentration of 1.4 mM, this detergent mimics the embedding of the proteins in native membranes. The DHPC concentrations used in this work (2–4 mM) maintained the integrity of the LH1 complexes at ambient pressure, but levels in excess of 10 mM DHPC resulted in degradation, as evidenced by the appearance of a $\alpha\beta$-$BChl_2$ heterodimer absorption band at ~820 nm. The DHPC-solubilized complexes remained stable under elevated pressures for at least 20 h at ambient temperature, which was more than sufficient for our trials. For complexes in their natural membrane environment, no detergent was added.

High-pressure spectroscopy

We acquired absorption spectra of isolated and membrane-bound LH complexes at ambient pressure and temperature using a V-570 spectrophotometer (Jasco) with a spectral resolution of 0.2 nm. We used a high-pressure diamond anvil cell (DAC) spectroscopy setup as previously

described, with a 0.35-mm-thick stainless-steel gasket preindented between the anvils under small pressure (24,25). A ruby-microbead pressure sensor (RSA Le Rubis SA) mounted directly into the sample volume was used to determine the pressure inside the DAC. The accuracy of the pressure measurements (defined as the pressure needed to shift the emission line at the output of the spectrograph by one pixel of the recording CCD camera) was 6.6 MPa. The temperature of the cell was maintained at 20 ± 0.5°C during the experiment, although there was very little alteration in the spectra when the temperature was varied between 18°C and 27°C. The pressure was changed stepwise with an average rate of 25–30 MPa per minute. The spectra, recorded with ~1 min acquisition time and spectral resolution of 0.56 nm per pixel, were measured with both increasing and decreasing pressure. As detailed below, the initial spectra were almost totally recovered upon pressure release. The spectra at each pressure were corrected by subtracting reference spectra that were measured in DAC filled with the pure buffer (or buffer-detergent) solvent.

Data analysis

The optical band parameters, position, and width, were determined by means of curve-fitting programs available in Origin (Microcal Software). In real measurements, the estimated accuracy (standard deviation (SD) within 95% confidence level) of the band position and width was 4–5 cm^{-1} (0.3–0.4 nm). For various samples, two to five repeat measurements were carried out to check the reproducibility of the measurements. A very good reproducibility of the data in the lower pressure region up to 1000 MPa was observed. However, above 1000 MPa, the reproducibility was poor because of the liquid-solid phase transition, which resulted in nonhydrostatic pressure distribution in the glassy protein sample. A slow residual red shift of the absorption band up to several nanometers was observed in the pressure region of protein denaturation, and the kinetics changed with pressure and temperature. We evaluated this potential source of experimental error on a control sample by prolonging the data acquisition time up to 100 min. The variations of the thus-deduced energetic parameters remained within the uncertainty limits determined by other factors. Therefore, and to avoid long-time protein deterioration, we stayed with the 1-min acquisition time.

RESULTS AND DISCUSSION

Overview optical absorption spectra of LH1 complexes at ambient conditions

The absorption spectra of the studied LH1 complexes shown in Fig. 2 reveal multiple bands in the wavelength range from 240 to 1000 nm. The broad band between 400 and 600 nm is primarily due to the carotenoids (spheroidene and spheroidenone) bound in the LH1 complex. The peaks at 375, 590, and 875 nm are related to electronic transitions in the BChl chromophores. As seen by comparison with the reference BChl spectrum, they correspond to the Soret, Q_x, and Q_y bands, respectively. The narrow band at ~280 nm belongs to the protein scaffold. Additional weak spectral features can be seen at 800 nm and ~760–770 nm in the samples containing RC complexes (curves 1–4); these are due to the monomeric BChl and bacteriopheophytin pigments in the RC.

Concentrating on the B875 absorption band, which peaks at ~875 nm, one can see that the spectral maxima of the membrane bound and isolated complexes almost coincide, with the exception of RC-LH1-PufX, where the membrane spectrum is 1.7 nm shifted to the red. It is also notable

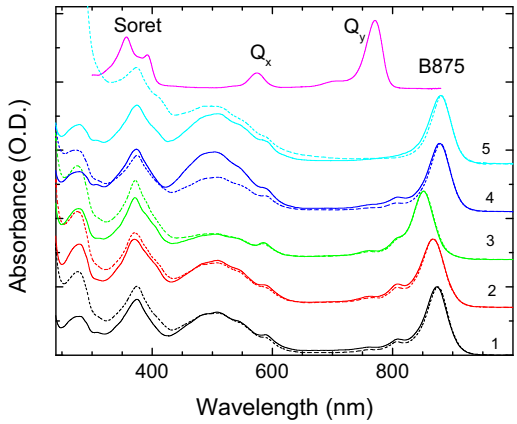

FIGURE 2 Absorption spectra of isolated (*continuous line*) and membrane (*dashed line*) complexes in buffer solution recorded at laboratory temperature and pressure: 1), RC-LH1-PufX; 2), β +9 mutant; 3), α +11 mutant; 4), RC-LH1; and 5), LH1-only. The curve on top represents the reference spectrum of Bchl in diethyl ether. The spectra, normalized with respect to the lowest-energy band peak, are shifted vertically relative to each other for better visibility.

that the spectral positions of the three membrane samples (LH1, RC-LH1, and RC-LH1-PufX) overlap within <2 nm despite their considerable structural differences. In agreement with published data (26–30), the mutation of the Trp residues in the RC-LH1-PufX complex to the Phe residues in positions β+9 or α+11 resulted in a blue shift (and broadening) of the absorption band by 7.1 (4.0) or 23.5 (1.2) nm in the case of membrane-bound complexes.

Remarkable pressure resistance of the membrane-bound complexes

Fig. 3 *A* displays a set of typical absorption spectra of a membrane-bound LH complex, in this case RC-LH1, responding to external high pressures. The B875 absorption band peak position and width (defined as the full width at half maximum (FWHM)) are presented in Fig. 3, *C* and *D*, respectively. The main pressure effect is a continuous red shift and broadening of the spectra, which is also seen for free BChl in solution (32). The measured shift and broadening rates, however, are very large compared with those obtained using free BChl. The very rapid initial shift of −1.04 ± 0.05 cm^{-1}/MPa (minus designates the shift to lower energies) observed in all membrane samples gradually diminishes with increasing pressure (Fig. 3 *C*). Similarly, the band broadening, with an initial rate of 0.24 ± 0.01 cm^{-1}/MPa, saturates past ~1000 MPa (Fig. 3 *D*). These large rates can be explained by the BChl-excited states in antenna complexes having an exciton origin (22,33,34). The shift and broadening rates measured for LH1 complexes are larger than those obtained for LH2 complexes (22–25), in agreement with the stronger exciton coupling in the core assemblies (35–38).

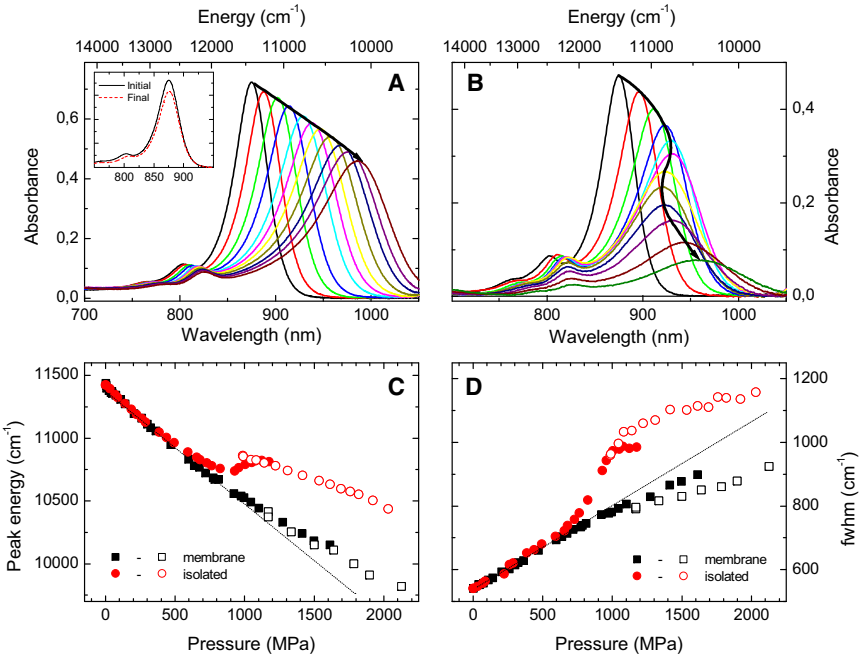

FIGURE 3 (*A* and *B*) Absorption spectra of membrane-bound (*A*) and isolated (*B*) RC-LH1 complexes as a function of pressure. The leftmost spectrum is recorded at ambient pressure; the pressure change between two successive spectra is 180 (*A*) or 160 (*B*) MPa. The arrowed bold lines follow successive absorption maxima. The inset demonstrates recovery of the shape of the ambient-pressure spectrum upon pressure release. (*C* and *D*) Pressure dependencies of the B875 exciton absorption peak position (*C*) and width (*D*) for the membrane-bound (*black squares*) and isolated (*red rings*) RC-LH1 complexes. The protein solutions solidify at pressures between 1200 and 1600 GPa, depending on the samples, which explains the increased noise and decreased reproducibility of the data toward the high end of the dependencies. Solid and open symbols represent data obtained in hydrostatic liquid and quasi-hydrostatic solid sample states, respectively. Dashed lines represent linear extrapolations of the membrane data to high pressures.

The inset of Fig. 3 *A* demonstrates an almost complete recovery of the spectrum upon pressure release at the completion of the cycle of measurements at elevated pressures. Some reduction of the spectrum intensity after decompression is unavoidable due to a spill-out of the sample from the high-pressure cell. Within the experimental precision, however, there are no signs of dissociation of the LH1 protein into smaller, dimeric and/or monomeric fragments, which would give rise to absorption peaks at 820 and 777 nm, respectively (39). Because most cytosolic oligomeric proteins are known to dissociate at pressures below 300 MPa (8), the native membrane-protected LH1 complexes are extremely pressure resistant.

Pressure-induced instability of detergent-isolated complexes: discontinuous shift and broadening of the B875 absorption band

Having established that the membrane-bound LH1 complexes exhibit extraordinary resilience at high pressures, we undertook experiments on LH1 complexes purified from their membrane environment and solubilized in detergent micelles above the critical micelle concentration.

Fig. 3 *B* shows the spectra of the detergent-isolated RC-LH1 complexes as a function of pressure. At low pressures up to ~500 MPa, the spectra behave in much the same way as the membrane-bound complexes. At higher pressures, however, initially the red shift begins to decrease in magnitude and then, between 700 and 1200 MPa, it is reversed with a blue shift. Past ~1200 MPa, the red shift is restored, albeit generally with a different rate, as can be seen in Fig. 3 *C*. A correlated abrupt spectral broadening occurs in the same pressure range of 700–1200 MPa, which implies a common physical origin of the shift and width behaviors. At low pressures, the absorption band of isolated complexes has almost the same width as it has in membrane-bound complexes. Toward higher pressures, the spectrum of isolated complexes broadens significantly, remaining broader than in membranes up to the largest pressures (Fig. 3 *D*). Fig. 3, *C* and *D*, demonstrate the strikingly different pressure responses of isolated complexes and membrane samples very visibly. Despite these differences, however, the recovery of the spectra of isolated complexes is almost as elastic as in the membrane-bound complexes (data not shown).

To enhance the variant behavior of isolated and membrane-bound complexes, we plotted the relative peak shifts $\Delta\nu$ and band broadenings $\Delta\delta$ (Fig. 4, *A* and *B*, respectively). The former measure is calculated as $\Delta\nu = \nu_i - \nu_m$, where $\nu_{i/m}$ are the corresponding experimental peak positions in isolated (i) and membrane-bound (m) samples. A blue shift of the spectrum of isolated complexes thus corresponds to a positive value of $\Delta\nu$. The latter quantity is in Gaussian approximation evaluated as $\Delta\delta = (\Gamma_i^2 - \Gamma_m^2)^{1/2}$, where $\Gamma_{i/m}$ are the corresponding FWHM for the B875 absorption bands. Spectral bandwidths are sensitive reporters of both static and dynamic disorders. The fact that Γ_i is always greater than Γ_m implies that membrane-bound complexes are generally more ordered than those isolated in detergent micelles.

In the background-free representation of Fig. 4, characteristic step-like dependencies resembling titration curves are shown for all complexes. The curves possess similar thresholds of ~700 MPa and midpoint pressures $\geq$1000 MPa, but rather different step heights for closed-ring (RC-LH1 and LH1) and open-ring (RC-LH1-PufX forms) structures above

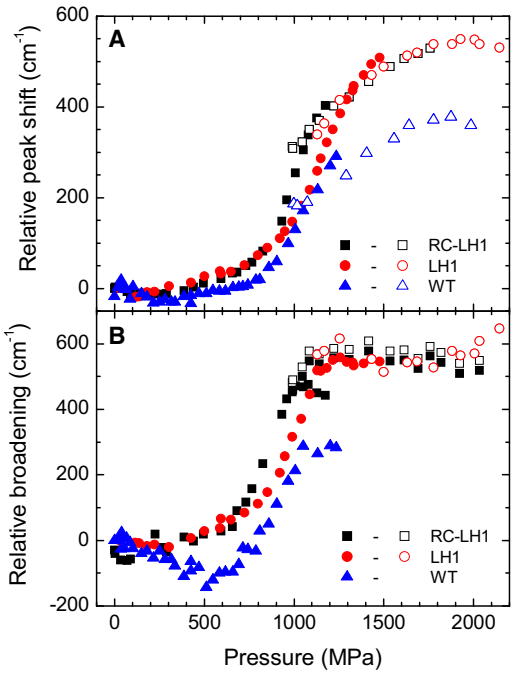

FIGURE 4 Relative peak shifts (*A*) and broadenings (*B*) of the B875 band in various LH1 complexes as indicated. WT denotes the RC-LH1-PufX complex. Solid and open symbols signify data obtained in liquid and solid phases, respectively. The overshooting data around 1000–1200 MPa are due to solidification of the sample and the accompanying drop of pressure in the course of measurements The ambient-pressure data corresponding to different complexes are drawn together for better comparison. In the case of WT complexes, this causes artificial negative values of the relative width at intermediate pressures. Due to excessive noise in the solid state, the broadening data are presented only for WT complexes in liquid.

1500 MPa. Thus, the height of the peak shift in the open-ring complexes reaches just ~2/3 that in the closed-ring samples. Similarly, the relative broadening (i.e., relative disorder) in the closed- and open-ring antennas behaves in a very different way. In the former complexes, only relative broadening is observed with increasing pressure until saturation above 1100 MPa, whereas in the latter, the absorption band of isolated complexes initially broadens more slowly than that of membrane-bound complexes (causing relative narrowing around 500 MPa) and starts to advance only past ~650 MPa. These features are consistent with the greater structural flexibility of the open-ring samples (discussed further below). The relatively wider (more extended) transition range along the pressure axis in the case of empty LH1-only rings also appears to be consistent with the results of an atomic force microscopy study (40), revealing a sizeable heterogeneity in both the size and shape of the detergent-purified LH1-only complexes, including circles, ellipses, and arcs.

The relative broadening of the spectra of isolated complexes is a sign of enhanced dynamics of the BChl molecules in the compressed binding sites of purified complexes, compared with the equivalent situation within the membrane. Because pressure-induced denaturation of proteins is driven by a decrease in volume and possible penetration of the buffer solvent (essentially of polar water molecules) into the protein interior (41–44), rather than swelling, the extra freedom of intraprotein movements can only be caused by breakage of the bonds that hold BChl molecules in their protein pocket. Given that axial ligation has a minimal effect on the BChl Q_y absorption band position (32), the loss of H-bonds in isolated complexes is the most likely explanation for the observed abrupt changes of their absorption spectra with pressure. Irregularities in the behavior of the RC-LH1-PufX complexes might be expected, given their open (and in the case of dimer, also bent (14)) structure, which may derive more stability from its membrane environment than monomeric closed-ring complexes. Modeling studies indeed indicate that the lipids surrounding RC-LH1-PufX distort to accommodate and stabilize the bent conformation of this complex (45).

Comparison of WT and H-bond mutant complexes

Under ambient conditions, a blue shift and broadening similar in magnitude to those seen in the pressure dependencies of the B875 absorption band (Fig. 4) were previously observed for H-bond mutants of *Rba. sphaeroides* compared with their WT counterparts (26–29). As can be seen from Fig. 1, the αTrp$_{+11}$ and βTrp$_{+9}$ protein residues normally bind BChls by forming H-bonds to the *C*3-acetyl carbonyls of the α- and β-BChls, respectively. Alteration of the Trp residues to Phe, which cannot form H-bonds, results in a total blue shift of the B875 absorption band by ~30 nm or 400 cm^{-1} in energy scale. The latter number agrees remarkably well with the height of the step for the relative shift in RC-LH1-PufX complexes seen in Fig. 4 *A*, suggesting that high pressure may indeed induce rupture of the H-bonds. To validate this mechanism, we studied two RC-LH1-PufX core complex mutants that have the H-bond Trp to Phe mutations in either the α +11 or β +9 positions in comparison with the WT RC-LH1-PufX sample. In the α+11 mutant, the H-bonds between the α polypeptides and its BChls are removed, and thus it has half the intact H-bonds found in the WT. In the β +9 mutant, the situation is exactly reversed: the H-bonds to β polypeptides are broken and the other H-bonds to α polypeptides are intact. The ambient-pressure spectra of these mutant samples shown in Fig. 2, which are blue shifted and broader than the reference spectra of WT complexes, are consistent with the published data (26).

In Fig. 5 *A*, the response to elevated pressures of the absorption peak position of the membrane-bound WT sample is compared with the two membrane-bound mutants. It would appear that the WT complex within the membrane resists the pressure and the H-bonds remain intact, whereas the mutant complexes, already destabilized by the loss of one set of H-bonds, undergo a gradual weakening and

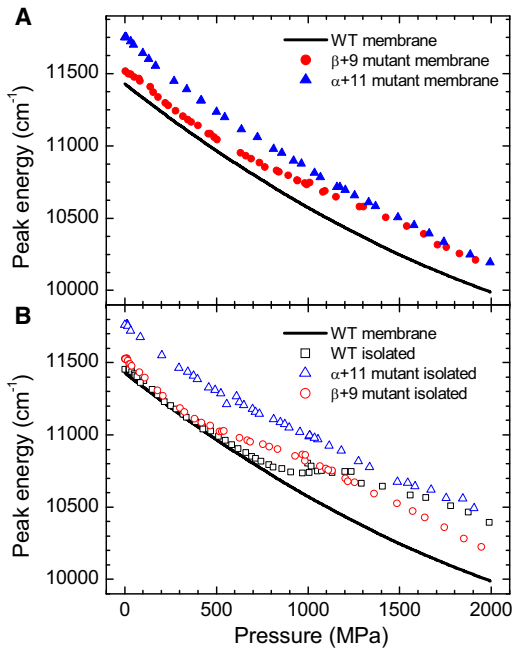

FIGURE 5 Comparisons of pressure dependencies of the B875 absorption peak for WT and mutant core complexes embedded in native membranes (*A*) or isolated in detergent micelles (*B*) See text for details.

finally disruption of the remaining H-bonds. In the case of the β+9-mutant, where the H-bonds between αTrp_{+11} and the α-bound BChl are intact, there is a transition to all broken H-bonds between ~500 and 1500 MPa. This fairly gradual transition may be due to a progressive distortion of the C-terminal helix of the α polypeptides (see Fig. 1), which might be anticipated for an open-ring structure, altering the geometry of the H-bonds, and lessening the extent of the blue shift imparted to the BChl. The α+11 mutant is constantly at a higher energy level, and almost parallel to the WT membrane, which may indicate that the original point mutation has caused a reorganization of the protein structure. This is highly likely, because the original Trp residues are considered membrane anchors, with the heterocyclic ring associating with polar lipid headgroups and the larger aromatic ring being buried among the hydrophobic lipid tailgroups. The Phe replacement residue is wholly hydrophobic and thus would be buried more deeply within the core of the membrane, altering the position of the α-polypeptide C-terminal helix with respect to the membrane interface. Studies of the exciton coupling constant modifications upon mutations, which will be reported elsewhere, confirm these speculations.

In Fig. 5 *B*, the responses of the membrane-bound and isolated WT complexes are compared with the isolated α+11 and β+9 mutant complexes. The mutants respond in much the same way as when they are in the membrane, although the α+11 mutant diverges more rapidly from the reference WT membrane beyond ~500 MPa (which may denote when the H-bonds to β polypeptides break), and the β+9 mutant does not quite reach the expected α+11 mutant level (which may be caused by compensating spectral shifts due to steric hindrance deformation of the chromophores). The most dramatic change, however, is seen for the detergent-purified WT complex, which demonstrates the breakage of both sets of H-bonds by approaching the α+11 mutant curve at ~1500 MPa. The synergistic structural role of the two sets of H-bonds is made clear by the much higher pressure that is necessary to induce a change in the spectral response of the WT at 700–800 MPa (see Fig. 4 *A*) compared with the β+9 mutant, which shows the first effects at <500 MPa.

Thermodynamic aspects of protein stability against pressure

The phenomenological basis of protein stability against pressure is well established (8–10). In the simplest version of thermodynamic modeling, only two global protein states, native (N) and denatured (D), are assumed. In the model presented here, the N state corresponds to the protein at ambient pressure, and the D state corresponds to its compressed state with broken H-bonds. The equilibrium constant of this two-state denaturation reaction is given by Eq. 1, where $[N]$ and $[D]$ indicate the concentrations of native and denatured protein, respectively; R is the universal gas constant; T is the thermodynamic temperature; and P is the pressure:

$$K(P) = \frac{[D]}{[N]} = \exp\left[\frac{-\Delta G(P)}{RT}\right] \quad (1)$$

In the lowest order approximation, the pressure dependence of the free-energy change associated with the protein denaturation can be represented as $\Delta G(P) = \Delta G^0 + \Delta V^0 P$, where $\Delta G^0 = G_D^0 - G_N^0$ is the standard free-energy difference between the denatured and native states, and $\Delta V^0 = V_D - V_N$ is the standard partial molar volume change between the states. For the protein to be stable, ΔG^0 has to be positive. If the volume of the denatured state is smaller than the volume of the native state (i.e., ΔV^0 is negative), the free-energy change decreases with increasing pressure. Past the transition midpoint pressure, $P_{1/2}$, the denatured state has lower free energy and is stabilized against the native state.

A connection of this minimalistic model with the spectroscopic experiment is established by calculating the pressure-dependent equilibrium constant as

$$K(P) = \frac{\Delta\nu(P) - \Delta\nu_i}{\Delta\nu_f - \Delta\nu(P)} \quad (2)$$

where $\Delta\nu(P)$ is the relative peak shift at pressure P (plotted in Fig. 4 *A*), and $\Delta\nu_i$ and $\Delta\nu_f$ are the shifts measured at initial (i) and saturating final (f) pressures, respectively. Inserting

Eq. 2 into Eq. 1 provides Eq. 3, a linear equation with respect to pressure:

$$-RT \ln K(P) = \Delta G^0 + \Delta V^0 P \quad (3)$$

The solution of Eq. 3 provides the prime model parameters, ΔV^0 and ΔG^0, as the slope and initial ($P = 0$) value, respectively. Additionally, $P_{1/2}$ can be found from the phase boundary condition: $\Delta G^0 + \Delta V^0 P_{1/2} = 0$.

The experimental pressure dependencies of $-RT\ln K$ for the isolated core complexes are shown in Fig. 6. The plots, which were built around the respective phase transition regions, are linear, reasonably justifying the applied model. With respect to the transition midpoint pressure, $P_{1/2}$ (crossing points of linear fitting curves with the y-axis zero), the complexes clearly divide into two groups with either one or two intact H-bonds in the basic unit. The three members of the latter group (LH1, RC-LH1, and WT) with midpoint pressures ≥ 1000 MPa demonstrate much greater pressure resistance than the two H-bond mutants with the midpoint pressures around 700 MPa. The slopes representing ΔV^0 do not separate that clearly.

The obtained parameters that characterize the pressure-induced rupture of H-bonds in detergent-isolated complexes, $P_{1/2}$, ΔV^0, and $\Delta G^0 = -\Delta V^0 P_{1/2}$, are listed in Table 1. Also included in Table 1 are the data for the membrane-bound β+9 mutant RC-LH1-PufX complex (line 5). Please note that the errors of the parameters in Table 1 represent SDs associated with the data points of individual measurements. The reproducibility measure of ensemble measurements is ill-defined due to the liquid-solid phase transition occurring at high pressures past ~1000 MPa (see "Data analysis" section for more details). It can be seen that comparable H-bond energies were found for purified and membrane-embedded β+9 mutant complexes (lines 4 and 5, respectively), suggesting that these integral membrane proteins largely retain their structural properties upon solubilization and purification in mild detergents. The parameters for the LH1, RC-LH1, and WT core complexes with all the H-bonds intact at ambient pressure appear similar, whereas they are rather different from those obtained for the mutant complexes with half of these bonds removed. Most remarkably, the energy corresponding to the H-bond rupture in the WT complex (25 ± 2 kJ/mol) equals within the estimated uncertainty the sum of the rupture energies in the α+11 and β+9 mutants (10 ± 2 and 14 ± 2 kJ/mol, respectively). This implies a quasi-independent role for the α- and β-types of H-bonds in reinforcing the $\alpha\beta$-$BChl_2$ building blocks and thus the whole LH1 complex.

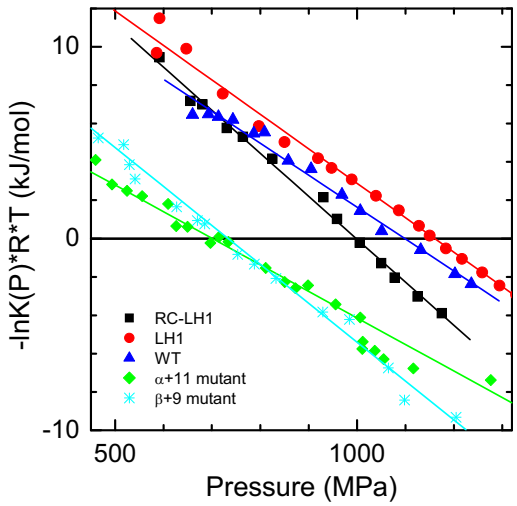

FIGURE 6 Dependencies of Eq. 3 for the detergent-isolated core complexes. The lines represent linear fits of the scattered experimental data.

TABLE 1 Thermodynamic parameters characterizing the breakage of H-bonds in core LH complexes

Sample	ΔG^0 kJ/mol	ΔV^0 ml/mol	$P_{1/2}$ MPa
LH1	21 ± 3	−18 ± 2	1160 ± 30
RC-LH1	25 ± 5	−25 ± 5	1000 ± 20
RC-LH1-PufX (WT)	25 ± 2	−23 ± 2	1090 ± 20
RC-LH1-PufX ($\beta Trp_{+9}Phe$)	14 ± 2	−20 ± 1	720 ± 20
RC-LH1-PufX ($\beta Trp_{+9}Phe$)*	14 ± 2	−15 ± 1	940 ± 20
RC-LH1-PufX ($\alpha Trp_{+11}Phe$)	10 ± 2	−14 ± 1	700 ± 30

*Parameters for mutant membrane, evaluated relative to the WT membrane.

CONCLUSIONS

Understanding the native and denatured states of membrane proteins allows one to gain insights into fundamental biological phenomena. By applying a unique combination of optical spectroscopy and genetic and noninvasive physical (high-pressure) engineering in this work, we were able to provide what is to our knowledge the first demonstration and quantification of the rupture of multiple H-bonds in the BChl-binding pockets of membrane chromoproteins with individual bond-type (α and β) selectivity. Although significant, concerted weakening and disruption of the H-bond network in water under pressure have been well documented (46,47), thus far, proof of similar reversible effects in proteins, particularly in membrane proteins, has been lacking.

We confirmed that H-bonds are essential for the structural stabilization of LH1 complexes, and are important for tuning their absorbance properties. We also established that the energy corresponding to rupture of H-bonds in the WT complex generally equals the sum of the rupture energies for the H-bonds in the α+11 and β+9 mutants. A similar roughly additive relationship between the absorption band shifts and the mutations made to the α- and β-polypeptides was previously observed by others (26,29).

A comparison of LH1 complexes in their native membrane and in a detergent-solubilized state also showed that the membrane bilayer plays a role as a stabilizing factor for this complex. Although comparable H-bond energies were found for purified and membrane-embedded β+9

mutant complexes, the removal of the complexes from the membrane clearly increased their vulnerability to applied pressure, as even the WT complex showed the breakage of both α and β sets of H-bonds. The notion that H-bonds are only one of the factors that play role in strengthening the proteins (48) is further supported by the extra stabilizing effect of the RC revealed by a comparison of the LH1-only complex with the RC-LH1 or RC-LH1-PufX complex: the LH1-only sample requires, on average, less energy to break the H-bonds (see Table 1).

The H-bond energies determined for the mutant complexes with just one set (α or β) of H-bonds intact appear to be only 4- to 6-fold greater than thermal energy at ambient temperature. This may not be enough for robust functioning of these proteins under harsh physiological conditions, which would explain the evolutionary design of the LH complexes with double H-bonds in the basic unit.

This work was partially supported by grants from the Estonian Ministry of Education and Science (No. SF0180055s07) and the Estonian Science Foundation (No. 8674 to A.F. and L.K.), the UK Biotechnology and Biological Sciences Research Council (C.N.H. and J.D.O.), and the Photosynthetic Antenna Research Center, an Energy Frontier Research Center funded by the Office of Science and Office of Basic Energy Sciences, U.S. Department of Energy (No. DE-SC0001035 to C.N.H.).

REFERENCES

1. Rose, G. D., and R. Wolfenden. 1993. Hydrogen bonding, hydrophobicity, packing, and protein folding. *Annu. Rev. Biophys. Biomol. Struct.* 22:381–415.
2. Polander, B. C., and B. A. Barry. 2012. A hydrogen-bonding network plays a catalytic role in photosynthetic oxygen evolution. *Proc. Natl. Acad. Sci. USA.* 109:6112–6117.
3. Bondar, A.-N., and S. H. White. 2012. Hydrogen bond dynamics in membrane protein function. *Biochim. Biophys. Acta.* 1818:942–950.
4. Sheu, S.-Y., D.-Y. Yang, …, E. W. Schlag. 2003. Energetics of hydrogen bonds in peptides. *Proc. Natl. Acad. Sci. USA.* 100:12683–12687.
5. Wendler, K., J. Thar, …, B. Kirchner. 2010. Estimating the hydrogen bond energy. *J. Phys. Chem. A.* 114:9529–9536.
6. Bowie, J. U. 2011. Membrane protein folding: how important are hydrogen bonds? *Curr. Opin. Struct. Biol.* 21:42–49.
7. Phelps, D. J., and L. K. Hesterberg. 2007. Protein disaggregation and refolding using high hydrostatic pressure. *J. Chem. Technol. Biotechnol.* 82:610–613.
8. Boonyaratanakornkit, B. B., C. B. Park, and D. S. Clark. 2002. Pressure effects on intra- and intermolecular interactions within proteins. *Biochim. Biophys. Acta.* 1595:235–249.
9. Silva, J. L., and G. Weber. 1993. Pressure stability of proteins. *Annu. Rev. Phys. Chem.* 44:89–113.
10. Scharnagl, C., M. Reif, and J. Friedrich. 2005. Stability of proteins: temperature, pressure and the role of the solvent. *Biochim. Biophys. Acta.* 1749:187–213.
11. Meersman, F., C. M. Dobson, and K. Heremans. 2006. Protein unfolding, amyloid fibril formation and configurational energy landscapes under high pressure conditions. *Chem. Soc. Rev.* 35:908–917.
12. Karrasch, S., P. A. Bullough, and R. Ghosh. 1995. The 8.5 A projection map of the light-harvesting complex I from *Rhodospirillum rubrum* reveals a ring composed of 16 subunits. *EMBO J.* 14:631–638.
13. Roszak, A. W., T. D. Howard, …, R. J. Cogdell. 2003. Crystal structure of the RC-LH1 core complex from *Rhodopseudomonas palustris*. *Science.* 302:1969–1972.
14. Qian, P., C. N. Hunter, and P. A. Bullough. 2005. The 8.5A projection structure of the core RC-LH1-PufX dimer of *Rhodobacter sphaeroides*. *J. Mol. Biol.* 349:948–960.
15. Fotiadis, D., P. Qian, …, C. N. Hunter. 2004. Structural analysis of the reaction center light-harvesting complex I photosynthetic core complex of *Rhodospirillum rubrum* using atomic force microscopy. *J. Biol. Chem.* 279:2063–2068.
16. Bullough, P. A., P. Qian, and C. N. Hunter. 2009. Reaction center-light-harvesting core complexes of purple bacteria. *In* The Purple Phototrophic Bacteria. C. N. Hunter, F. Daldal, M. C. Thurnauer, and J. T. Beatty, editors. Springer, Dordrecht, The Netherlands.
17. Pugh, R. J., P. McGlynn, …, C. N. Hunter. 1998. The LH1-RC core complex of *Rhodobacter sphaeroides*: interaction between components, time-dependent assembly, and topology of the PufX protein. *Biochim. Biophys. Acta.* 1366:301–316.
18. Jamieson, S. J., P. Wang, …, P. A. Bullough. 2002. Projection structure of the photosynthetic reaction centre-antenna complex of *Rhodospirillum rubrum* at 8.5 A resolution. *EMBO J.* 21:3927–3935.
19. Adams, P. G., and C. N. Hunter. 2012. Adaptation of intracytoplasmic membranes to altered light intensity in *Rhodobacter sphaeroides*. *Biochim. Biophys. Acta.* 1817:1616–1627.
20. Freiberg, A., A. Ellervee, …, K. Timpmann. 1993. Pressure effects on spectra of photosynthetic light-harvesting pigment-protein complexes. *Chem. Phys. Lett.* 214:10–16.
21. Sturgis, J. N., A. Gall, …, B. Robert. 1998. The effect of pressure on the bacteriochlorophyll *a* binding sites of the core antenna complex from *Rhodospirillum rubrum*. *Biochemistry.* 37:14875–14880.
22. Timpmann, K., A. Ellervee, …, A. Freiberg. 2001. Short-range couplings in LH2 photosynthetic antenna proteins studied by high hydrostatic pressure absorption spectroscopy. *J. Phys. Chem. B.* 105:8436–8444.
23. Gall, A., A. Ellervee, …, B. Robert. 2003. Membrane protein stability: high pressure effects on the structure and chromophore-binding properties of the light-harvesting complex LH2. *Biochemistry.* 42:13019–13026.
24. Kangur, L., K. Timpmann, and A. Freiberg. 2008. Stability of integral membrane proteins under high hydrostatic pressure: the LH2 and LH3 antenna pigment-protein complexes from photosynthetic bacteria. *J. Phys. Chem. B.* 112:7948–7955.
25. Kangur, L., K. Leiger, and A. Freiberg. 2008. Evidence for high-pressure-induced rupture of hydrogen bonds in LH2 photosynthetic antenna pigment-protein complexes. *J. Physics: Conf. Series.* 121:112004.
26. Olsen, J. D., G. D. Sockalingum, …, C. N. Hunter. 1994. Modification of a hydrogen bond to a bacteriochlorophyll a molecule in the light-harvesting 1 antenna of *Rhodobacter sphaeroides*. *Proc. Natl. Acad. Sci. USA.* 91:7124–7128.
27. Olsen, J. D., J. N. Sturgis, …, B. Robert. 1997. Site-directed modification of the ligands to the bacteriochlorophylls of the light-harvesting LH1 and LH2 complexes of *Rhodobacter sphaeroides*. *Biochemistry.* 36:12625–12632.
28. Sturgis, J. N., J. D. Olsen, …, C. N. Hunter. 1997. Functions of conserved tryptophan residues of the core light-harvesting complex of *Rhodobacter sphaeroides*. *Biochemistry.* 36:2772–2778.
29. Uyeda, G., J. C. Williams, …, J. P. Allen. 2010. The influence of hydrogen bonds on the electronic structure of light-harvesting complexes from photosynthetic bacteria. *Biochemistry.* 49:1146–1159.
30. Freiberg, A., K. Timpmann, and G. Trinkunas. 2010. Spectral fine-tuning in excitonically coupled cyclic photosynthetic antennas. *Chem. Phys. Lett.* 500:111–115.
31. Jones, M. R., G. J. S. Fowler, …, C. N. Hunter. 1992. Mutants of *Rhodobacter sphaeroides* lacking one or more pigment-protein complexes and complementation with reaction-centre, LH1, and LH2 genes. *Mol. Microbiol.* 6:1173–1184.

32. Ellervee, A., and A. Freiberg. 2008. Formation of bacteriochlorophyll a coordination states under external high-pressure. *Chem. Phys. Lett.* 450:386–390.

33. Wu, H.-M., M. Rätsep, …, G. J. Small. 1997. Comparison of the LH2 antenna complexes of *Rhodopseudomonas acidophila* (strain 10050) and *Rhodobacter sphaeroides* by high-pressure absorption, high-pressure hole burning, and temperature-dependent absorption spectroscopies. *J. Phys. Chem. B.* 101:7641–7653.

34. Wu, H.-M., M. Rätsep, …, G. J. Small. 1998. Hole-burning and absorption studies of the LH1 antenna complex of purple bacteria: effects of pressure and temperature. *J. Phys. Chem. B.* 102:4023–4034.

35. Timpmann, K., G. Trinkunas, …, A. Freiberg. 2005. Excitons in core LH1 antenna complexes of photosynthetic bacteria: evidence for strong resonant coupling and off-diagonal disorder. *Chem. Phys. Lett.* 414:359–363.

36. Timpmann, K., G. Trinkunas, …, A. Freiberg. 2004. Bandwidth of excitons in LH2 bacterial antenna chromoproteins. *Chem. Phys. Lett.* 398:384–388.

37. Pajusalu, M., M. Rätsep, …, A. Freiberg. 2011. Davydov splitting of excitons in cyclic bacteriochlorophyll a nanoaggregates of bacterial light-harvesting complexes between 4.5 and 263 K. *ChemPhysChem.* 12:634–644.

38. Sener, M., J. Hsin, …, K. Schulten. 2009. Structural model and excitonic properties of the dimeric RC-LH1-PufX complex from *Rhodobacter sphaeroides*. *Chem. Phys.* 357:188–197.

39. Loach, P. A., and P. S. Parkes-Loach. 2008. Structure-function relationships in bacterial light-harvesting complexes investigated by reconstitution techniques. *In* The Purple Photosynthetic bacteria. C. N. Hunter, F. Daldal, M. C. Thurnauer, and J. T. Beatty, editors. Springer, Dordrecht, The Netherlands. 181–198.

40. Bahatyrova, S., R. N. Frese, …, J. D. Olsen. 2004. Flexibility and size heterogeneity of the LH1 light harvesting complex revealed by atomic force microscopy: functional significance for bacterial photosynthesis. *J. Biol. Chem.* 279:21327–21333.

41. Chryssomallis, G. S., P. M. Torgerson, …, G. Weber. 1981. Effect of hydrostatic pressure on lysozyme and chymotrypsinogen detected by fluorescence polarization. *Biochemistry.* 20:3955–3959.

42. Collins, M. D., G. Hummer, …, S. M. Gruner. 2005. Cooperative water filling of a nonpolar protein cavity observed by high-pressure crystallography and simulation. *Proc. Natl. Acad. Sci. USA.* 102:16668–16671.

43. Harano, Y., T. Yoshidome, and M. Kinoshita. 2008. Molecular mechanism of pressure denaturation of proteins. *J. Chem. Phys.* 129:145103.

44. Roche, J., J. A. Caro, …, C. A. Royer. 2012. Cavities determine the pressure unfolding of proteins. *Proc. Natl. Acad. Sci. USA.* 109:6945–6950.

45. Hsin, J., J. Gumbart, …, K. Schulten. 2009. Protein-induced membrane curvature investigated through molecular dynamics flexible fitting. *Biophys. J.* 97:321–329.

46. Jonas, J., T. DeFries, and D. J. Wilbur. 1976. Molecular motions in compressed liquid water. *J. Chem. Phys.* 65:582–588.

47. Cunsolo, A., F. Formisano, …, S. Finet. 2009. Pressure dependence of the large-scale structure of water. *J. Chem. Phys.* 131:194502.

48. Todd, J. B., P. A. Recchia, …, P. A. Loach. 1999. Minimal requirements for in vitro reconstitution of the structural subunit of light-harvesting complexes of photosynthetic bacteria. *Photosynth. Res.* 62:85–98.